

Introduction of SPELEEM at BL17SU/SPring-8

M. Kotsugi and F.Z. Guo

2007.09.10

Photoelectron emission microscope (PEEM) has been of great benefit in the field of surface science. PEEM provides the spatial distribution of photoemitted electron with the resolution power of several ten nanometers [1]. Especially, a combination technique with synchrotron radiation (SR) enables us to visualize a magnetic domain image using magnetic circular dichroism (MCD) or magnetic linear dichroism (MLD) effect: for example, anti-ferromagnetic domain imaging in NiO [2], exchange bias effect at magnetic multilayer [3] or magnetization flipping dynamics in magnetic thin film [4]. Here, we will present the operation principle of PEEM with mentioning several successful results.

The spatial distribution of photoemitted electron is primarily magnified by the large difference in electric potential between sample and objection lens (on the order of 20kV), and the repeat of column and projection lenses produces the final magnified image on the screen with the magnification power of about 10^4 . The photoelectron intensity emitted from the surface is proportional to the x-ray absorption intensity; therefore spatially resolved x-ray absorption fine structure (XAFS) is projected on each pixel in the screen. XAFS spectrum does not lead only the chemical composition but also crystallographic structure, electronic structure and magnetic domain structure. The height of absorption edge in XAFS is proportional to the chemical composition, and the fine structure near absorption edge represents the electronic structure and chemical bonding state of photoemitted atom. The continuous scanning of the photon energy towards extended region of absorption edge also provides the information of crystallographic structure [5]. Furthermore, the difference in the absorption intensity depending on the polarization of synchrotron radiation provides the magnetic domain structure using the principle of a magnetic optical Kerr effect so called as magnetic circular dichroism or linear dichroism (MCD, MLD) [6, 7]. The electric vector of synchrotron radiation strongly correlates with magnetic moment, and it represents in the obtained intensity of photoelectron. In this way, these solid-state properties are obtained on each pixel in viewing field on PEEM.

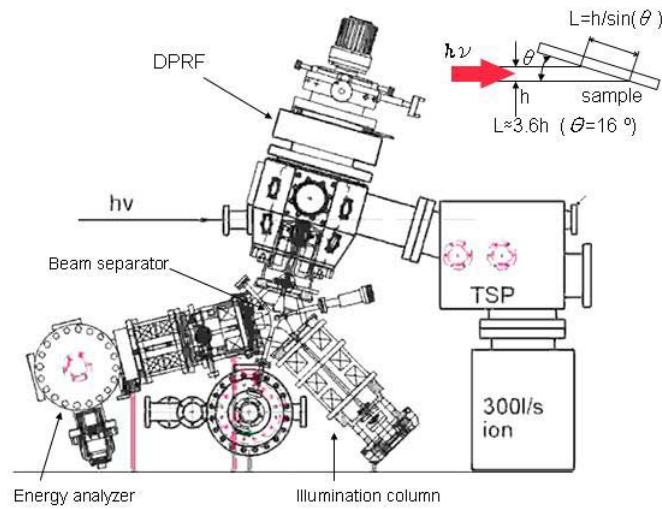


Fig. 1. Side view image of the SPELEEM instrument installed in SPring-8. Upright configuration and DPRF are the key features.



Fig. 2. Front view of the SPELEEM instrument. 1, manipulator, 2, photon incident port, 3, quadrupole mass spectrometer, 4, projector column, 5, energy analyzer, 6, image column, 7, Hg lamp, 8, preparation chamber, 9, air lock, 10, sputter ion gun.

Figure 1 and 2 show the side view and front view of SPELEEM (Spectroscopic PhotoEmission and Low Energy Electron Microscope), respectively. It is composed of manipulator, analysis room, and magnetic type 60-degree beam separator, electron beam irradiation column, image column, energy analyzer, projection lens column, and preparation room [8]. On the sample manipulator, Tilt of $\pm 3^\circ$ in a horizontal plane can be adjusted. Sample position can be precisely adjusted for XYZ motion in the ultrahigh

vacuum. To apply a high voltage of 20 KV on the sample, the HV cable for that is introduced from the outside into the inside of the manipulator, and it is connected with the current introduction electrode. There is one sample stage in the sample preparation room, and the reserve of the sample can be heated. Moreover, because the sputter ion gun is installed, it is possible to use it to make the sample surface clean. It is being equipped with mass analyzer (Q-mass) in the analysis room, and it is used to inspect the residual gas. Moreover, it is possible to deposit to the surface of the sample at the observation position by evaporation sources (EFM). This deposition source can be separated from the analyzer by retracting it with the gate valve. Even if the analysis room is not atmospheric opened, the deposition sources can be exchanged because each EFM can be independently exhausted. SPELEEM instrument is put on three axis driving trestle to adjust the best position of the XPEEM observation of the focus of a sample and incidence X rays because of the motor drive. The sample can be cooled down to 150K by liquid nitrogen. Moreover, the sample can be heated by radiation heating, electron beam impact heating, and direct energizing heating is also possible. In case of the radiation heating 900K is possible, in case of electron beam impact heating 1,900K is possible.

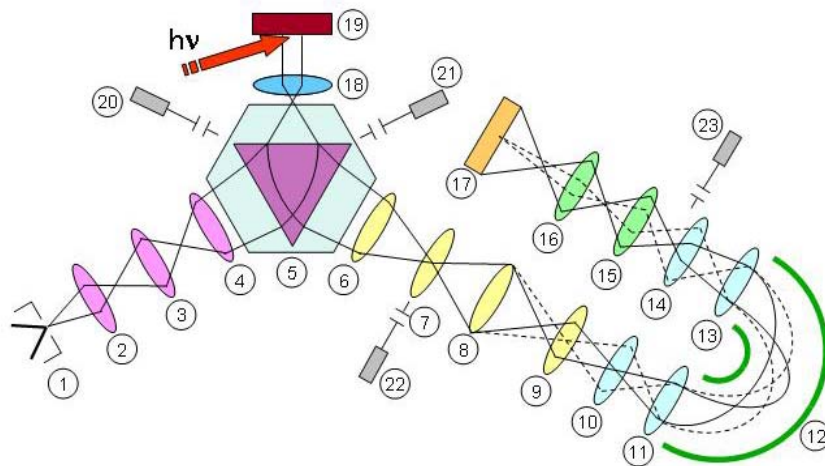


Fig. 3. Electronic optics system of SPELEEM.

The diagram of an electronic optics system is shown in Fig. 3. The main composition is as follows.

- 1, The electron beam irradiation system composed of three capacitor lens and the electronic irradiation gun. (1 - 4)
- 2, Beam separator in which irradiation electron beam is reflected by 120° , and focusing is effective. (5)

- 3, Object lens (L1) located in front of sample.
- 4, Image column (L2 - L5) that composes of lens (forwarding lens, field lens, middle lens, and one projection lens).
- 5, Energy analyzer (L6 - L10) that composes of obstruction lens, image lens (L6), hemisphere analyzer, acceleration lens, and image lens (L10).
- 6, Projection lens system (L11 - L12) composed of the two projection lenses.

It equips the deflector in front of all lenses to correct the beam orbital. The energy slit is located at the exit slit of a hemisphere analyzer, this plane is also corresponds to the energy dispersion plane. The energy width of the slit is 0.3 eV. It enables us not only to decrease the chromatic aberration, but also to resolve the kinetic energy of photoelectrons. The pass energy of the energy analyzer is 1 keV. Three apertures (incidence aperture of the electron beam, field aperture, and contrast aperture) are installed in the each beam separator and the field lens.

To project the low-speed electron emitted or reflected from the surface of the solid, it is necessary to accelerate into high energy in object lens. It arises the very large aberration added by the acceleration electric field of the first objective lens. Object lens is composed of three-pole lens with the magnetic field operation, and it is 20keV with electric field of 10kV/mm. For the electron with the initial energy of 10eV and the width of 0.5 (0.1) eV, theoretical best resolution is calculated as 5 (3) nm. The spatial resolution is decided for SPELEEM by an electronic optics system. The aberration that restricts the spatial resolution of the microscope is a spherical aberration chiefly, a chromatic aberration, and a diffraction aberration. The spherical aberration and the chromatic aberration should consider growing of the diffraction aberration of the electron oppositely if it squeezes it too much by squeezing contrast aperture for the aberration and the contrast adjustment that exists in the field lens though it becomes small. The energy resolution is decided depending on both the energy resolution of synchrotron radiation and the energy resolution of the energy analyzer. Actual spatial resolution also receives the influences of other experimental factors, for instance, the kind of the sample, the currents of the lens, the high voltage stabilities, and the adjustment situations, etc. It is necessary to correct the aberration of the beam separator and object lens (chromatic and spherical aberration) to aim at higher resolution by a more complex means.

There are three kinds of basic functions of SPELEEM (an image mode, a diffraction mode, and a decentralized mode). In all modes, the lens to the middle lens is similarly operated. The operation mode can be switched by the change of the lens settings after

intermediate lens and a suitable aperture setting. In LEEM mode, incident electron beam is bent with the beam separator, and it is decelerated rapidly from 20 keV just before the sample. After the reflection at the sample surface, electron is accelerated again to 20 keV. The accelerated electron beam is bent with the beam separator again, and reaching the image column, and passing the analyzer, and projected to the screen at the end. In addition, the electron beam that is reflected on the surface forms the LEED(low Energy Electron Diffraction) pattern on focal plane in object lens. The LEED pattern is forwarded to the field lens with the beam separator and the transfer lens.

The electron trajectory of diffraction mode is presented as dot line in Fig. 3, and the electron trajectory of image mode is also presented as solid line. By adjusting the current of the intermediate lens, the position of focal plane and the image plane is changed, and switching from the image mode to the diffraction mode is finally achieved. The LEED pattern of the local area is obtained by choosing field aperture that exists in incidence aperture and the beam separator of the electronic irradiation system. There are three sizes (200 μm and 100 μm and 20 μm) infield aperture. According to the expansion rate of objective lens and the selection of aperture, the minimum selection area on the sample will be estimated as 896 nm.

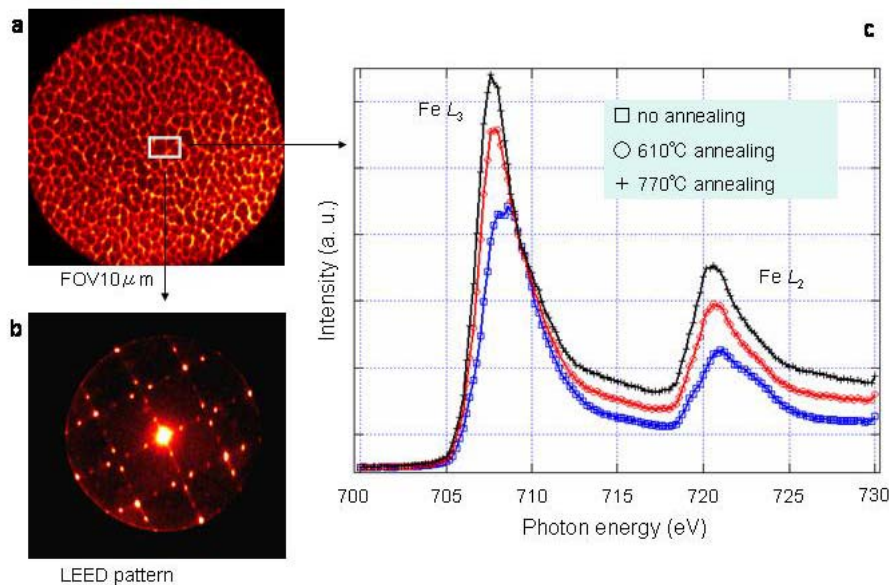


Fig.4, (a)Mirror image of iron oxide with field of view 10 micro-meter. (b)LEED pattern of a selected region of the iron oxide. (c)Nano-XANES of a selected region of the iron oxide obtained at different annealing temperature.

The phase contrast and the diffraction contrast arise from the periodicity of crystallographic structure is the most important mechanism of LEEM. MEM(Mirror

ElectronMicroscope) is one of the special modes using an electron beam. An incident electron can be reflected without invading the sample by adjusting the potential of the sample lower than that of the electron gun. MEM can be useful for the research of the sample without the diffraction and the interference contrast, and the potential distribution on the surface of the sample, the surface electric field, and the image of the magnetic field distribution be acquired. Because the MEM image sees the contrast that originates in an electric field on the surface of the sample not uniform, the surface need not clean be made like LEED and LEEM, etc.

To use SPELEEM as XPEEM in the connection of synchrotron radiation, the electron beam irradiation part is not used. The Wehnelt potential is concretely adjusted to stop incidence electron beam, and, instead, light is irradiated to the sample. In the imaging of the photoelectron emitted from the sample, the setting of the forwarding lens, the projection lens, and the analyzer in the LEEM mode is maintained as it is. The photoelectron that passes the energy analyzer is selected by the potential adjustment of the sample. Because the electric field between object lens changes when the potential of the sample changes, the focus gives a little adjustment to the current of object lens to match it. In the use of synchrotron radiation, photon energy can be arbitrary selected as we want, it is the key XPEEM. The element specific image is obtained by choosing the core level of arbitrary element. Moreover, complete x-ray absorption spectrum on the local area can be obtained by continuous image acquisition with sweeping the photon energy. If the transmission of the electron optical system is sacrificed, resolution is improved by inserting Contrast aperture because the photoelectron has a wide range of the angle and a wide energy distribution. Field of view in the image mode is possible to change from 100 μm to 2 μm .

In summary, each mode of PEEM, LEEM, and LEED can be selected according to the necessity of the experiment, and photoelectric diffraction (PED) in MEM or the local domain and value electronic angle distribution (VPEAD) measurement are used for others in SPELEEM assisting as described above. The atomic structure and the electronic structure in the local area can be investigated using these various measurement modes well.

A magnetic domain observation of the magnetic multilayer film using circular and linear polarized synchrotron radiation is one of the most popular use of PEEM now in worldwide. It will be characterized a kind of magneto optical Kerr effect (MOKE) that arose from the polarization of synchrotron radiation (photon spin) and magnetic moment of the specimen.

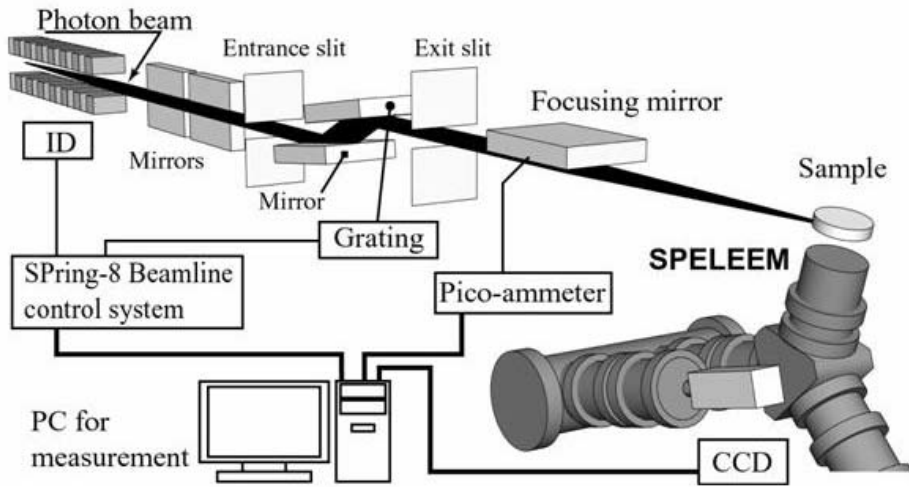


Fig. 5, Schematic of the experimental configuration.

Figure 5 shows the schematic of experimental configuration of SPELEEM at soft x-ray beamline. The CCD camera, pico-ammeter and the SPring-8 control system are controlled simultaneously. The SPELEEM is installed at BL17SU/SPring-8, in which photons with a wide energy range and multi-polarizations are produced. BL17SU is the first beamline in SPring-8 to employ a multi-polarization mode undulator, which is composed of electromagnet arrays and permanent magnet arrays [9]. Horizontal or vertical linearly polarized light can be selected by phasing the permanent magnet arrays or changing the current of the electromagnets, whereas left or right circularly polarized light can be obtained by changing the polarity of the current in the electromagnets. Photon energies from 250 eV to 2000 eV are available. This wide photon energy range covers the K -edges of elements including C, N and O, the L -edges of 3d transition-metal elements, and M -edges of 4f rare earth elements. The photon flux is higher than 10^{11} photons/s, while the energy resolution is $E/\Delta E > 10$ [10].

An intense photoelectron signal is necessary to reach a higher lateral resolution. Hence, we introduced refocus optics that employ horizontally coplanar sagittal and tangential focusing cylindrical mirrors to produce a 15:1 demagnified image at the exit slit. A focused x-ray spot for a 50 μ m exit slit is shown in Fig. 6. The profiles for the horizontal and vertical directions are also plotted. The field of view of the image is 50 μ m. The illuminated size is estimated through the half maximum of profile peaks to be 14.3 μ m in the horizontal direction and 14.6 μ m in the vertical direction. Considering the impinging angle of 16 degrees to the sample because of the upright configuration, the actual x-ray size is estimated to be $14 \times 3 \mu$ m². This x-ray size is effective because

the illuminated area on the sample is almost round; thus, we can obtain XPEEM images at a field of view of $10 \mu\text{m}$ without changing the x-ray position [11]. This focused x-ray allows us to obtain clear XMCD contrasts of permalloy patterns at a size of 200 nm even for a short acquisition time of 0.5 sec .

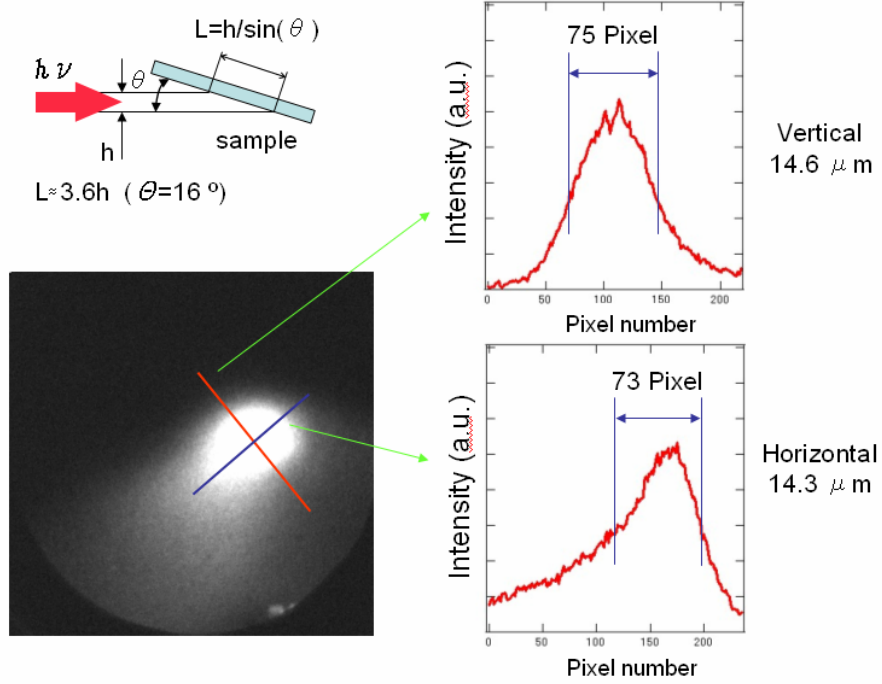


Fig. 6, Focused x-ray spot profile. The illuminated area is estimated through the half maximum of profile peaks to be $14.3 \mu\text{m}$ in the horizontal direction and $14.6 \mu\text{m}$ in the vertical direction, respectively.

The x-ray absorption intensity changes depending on the polarization of the synchrotron radiation. The amount of absorbed X rays increases when photon spin of the circular light and magnetic moment is in parallel configuration, and it also decreases in anti-parallel configuration. For instance, let's think about $2p\text{-}3d$ excitation of the transition metal. Pattern diagram of partially occupied $3d$ orbital is shown in Fig. 4a, with which is specified as azimuthal quantum number of $+2, +2, 0, -2, -2$, and also for spin moment of $1/2$, and $-1/2$. Optical spin is indicated as σ^+, σ^- . The cross section of $3d$ electron respect to each circularly polarized light and the linear polarization is shown for each azimuthal quantum number in Figure 7, b), c), and d). For magnetized elements, dipole transition is caused by the spin-orbital interaction, and the asymmetric diversity is caused in the transition probability, in a word, MCD strength for a magnetic atom, and the difference in this cross section caused in the asymmetry, namely MCD intensity. This cross section is proportional to the second power of the Clebsch-Gordon

coefficient. The ferromagnetic domain having parallel magnetic moment respect to photon spin is observed brightly in PEEM screen, and also that of anti-parallel domain is observed darkly. By the way, the magnetic domain in 90 degree configuration is observed as the gray, because the right and left of the magnetization cannot be distinguished. To distinguish this two domain, it only has to measure in a different azimuth angle. Moreover, the anti-ferromagnetic domain can be observed by line dichroism (MLD) using the linear polarization synchrotron radiation in similar manner. Figure 8 shows examples of anti-ferro magnetic domains structures and ferro magnetic domain structures, respectively.

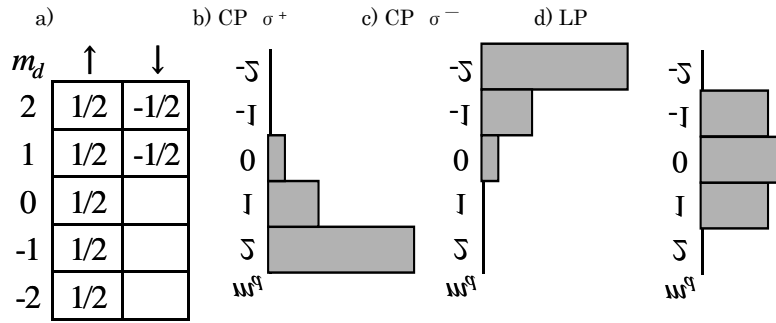


Fig. 7, (a)d-electron occupied states of transition metal. (b) b),c) Cross section of 3d orbital for each quantum number respect to each circularly polarized light. d) Cross section for linearly polarized light.

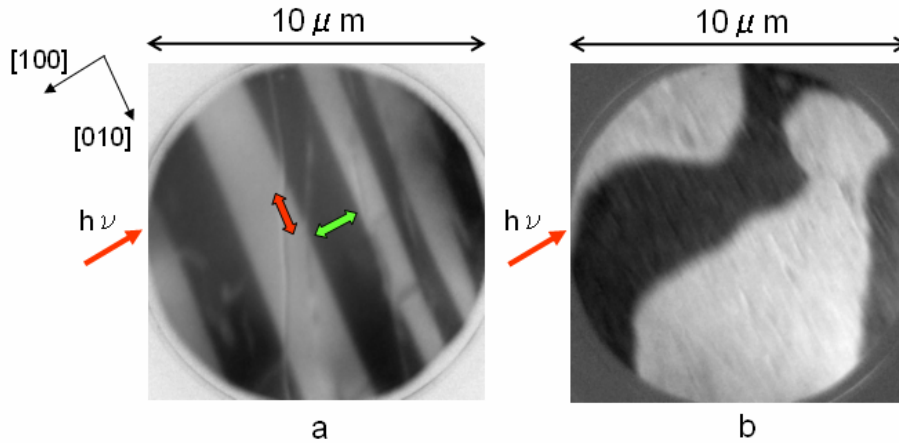


Fig. 8, (a) XMLD image of a bare NiO(001) and (b) XMCD image of an Fe single crystal.

Moreover, the in-plane and out-of-plane magnetization can be distinguished by rotating azimuth angle. For out-of-plane magnetization, the angle between photon spin and magnetic moment doesn't change by the azimuth rotation, if contrast in magnetic

domain changes, it should have in-plane magnetization. Information on a magnetic moment of each element can be obtained by selecting the light energy of the excitation light. In addition, relative ratio between spin and the orbit moment can be analyzed by applying the spin sum rule to the MCD spectrum obtained by scanning light energy. This analysis can be applied on each pixel of viewing field, therefore, information of local magnetic moment can be directly obtained. This technique is being typical use now to understand a magnetic domain structure of magnetic multilayer, but also various related magnetic substances.

- [1] J. Stöhr et al., Surf. Rev. Lett. **5** (1998) 1297.
- [2] F. U. Hillebrecht et al. Phys. Rev. Lett. **86** (2001) 3419.
- [3] W. Kuch et al., Nature Materials **5** (2006) 128.
- [4] K. Fukumoto et al., Phys. Rev. Lett. **96** (2006) 097204.
- [6] Stöhr, J., et al., Surf. Rev. Lett. **5** (1998) 1297.
- [7] Kuch, W., et al., Nature Mater. **5** (2006) 128.
- [5] Kotsugi, M., et al., e-J. Surf. Sci. Nanotechnol. **4** (2006) 490.
- [8] F. Z. Guo et al., J. Phys.: Condens. Matter **17** (2005) S1363.
- [9] K. Shirasawa, T. Tanaka, T. Seike, A. Hiraya, and H. Kitamura, AIP Conference proceedings **705** (2003) 203 The 8th SRI.
- [10] H. Ohashi, *et al.*, AIP Proc. **879** (2007) 523.
- [11] F. Z. Guo et al. Rev. Sci. Instrum. **78** (2007) 066107.